INTERNATIONAL JOURNAL OF GEOMATICS AND GEOSCIENCES
Volume 8, No 1, 2018

Research article ISSN 0976 – 4380

Deformational features of intraformational para-conglomerate of the Paleoproterozoic Sanvordem Formation, Goa Group indicates a brittle-ductile dextral shear

Gadgil R[1], Miranda M. A[2], Viswanath T. A[3]
1, 2, 3- Department of Earth Science, Goa University, Taleigao Plateau, Goa
geology.raghav@unigoa.ac.in

ABSTRACT

Structures at outcrop and microscale have been studied of an intraformational para-conglomerate that belongs to the basal section of Sanvordem Formation of the Goa Group of rocks. The mylonitic foliation plane is sub vertical striking NNW-SSE with steep easterly dips. High viscosity contrast between the clasts and the chlorite-biotite rich matrix have rendered a unique texture to the rocks. The elliptical rounded to subrounded microscopic to boulder size clasts have been flattened and subjected to subsequent shearing. Outcrop scale structures abound in mantled clasts with "bearded" and recrystallized "tails" along with detached/stretched pebbles parallel to foliation. Chlorite-biotite rich matrix has suffered maximum deformation and recrystallization. Quartz grains show high degree of internal strain as evidenced by undulatory extinction and subgrain formation. Quartz fish and ribbons also occur abundantly. The quartzofelspathic clasts are rimmed by dynamically recrystallized finer grained mineral aggregates. Mantled lithoclasts indicate ductile deformation in response to flow in the matrix. The porphyroclasts of quartz, alkali feldspar and calcite are round to sigmoid in outline with beards of neocrystallized fibrous minerals i.e. muscovite, chlorite, quartz and calcite. However, these minerals also exhibit effects of brittle deformation such as displaced twin lamellae in plagioclase and microfaulting of quartz and calcite porphyroclasts. The structures indicate Top-to-E (down) dextral shear. Microscopic structural features have been used as temperature gauges. Width of twinned lamellae in calcite, ductile behavior of biotite, brittle fracturing of plagioclase and alkali feldspar, dynamic recrystallization and BLG in quartz, indicate that the rock has undergone mylonitization occurring at a transition zone of brittle-ductile regime within a temperature range of 200-450° C.

Keywords: para-conglomerate, shear zone, Sanvordem Formation, Goa Group, dextral shear.

1. Introduction

Analysis of deformed rocks qualify to be one of the few direct sources of information available for the reconstruction of tectonically deformed areas. Shear zones are widely used for studying deformation characteristics of an area (Ramsay, 1980; Ramsay & Graham, 1970). Deformation in a shear zone causes development of characteristic fabrics and mineral assemblages that reflect P-T conditions, type of flow, sense of movement and history of deformation in a shear zone (Passchier & Trouw, 2005). A very important process that is characteristic of shear zones gives rise to rocks called as 'mylonites'. Mylonite zones can form in any rock type and they span from sub-millimeter scale to zones several km wide (Bak, et al., 1975; Hanmer, 1988). Study of deformed objects of known initial shape appears fruitful (Ramsay, 1967). Deformed conglomerates typically fall into this category. In case of coexistence of 'hard' and 'soft' minerals, the hard minerals exhibit rotation in the flow of the soft material and may also get stretched. Similar rule of rheology applies for lithoclasts of hard rocks floating in a soft micaceous matrix. These hard minerals form porphyroclasts that deform giving rise to the sense of shear.

The intraformational para-conglomerate under study occurs as discontinuous outcrops and is exposed in central Goa in a NW-SE stretch of about 30 km from Sanvordem in the southeast to Panjim in northwest. It has been mapped and studied for outcrop and microstructural data in and around Sanvordem town (Figure 1). Detailed structural studies on this para-conglomerate including both outcrop scale and microscale observations were unavailable till date, except for brief descriptions of microstructures (Devaraju, et al., 2010; Rekha, et al., 2013a; Gadgil, et al., 2015) and monazite dating of clasts and matrix in these rocks (Rekha, et al., 2013a). Absence of faceted and striated boulders in this para-conglomerate rules out any possibility of glacial origin (Gokul, et al., 1985). The present study aims at understanding the detailed textures and structures of the para-conglomerate and provide an insight on the shear sense developed.

2. Geological setting and field structures

The study area (Figure 1) lies at the central portion of Sanguem Taluka of Goa. The rock types present in this area are polymict para-conglomerates which occur as narrow lensoid bands within the metagreywackes (Gokul, et al., 1985) that represents the oldest member of the Sanvordem Formation. Due to its highly irregular and lensoid occurrence in greywacke, lack of any sorting and larger "matrix: clast" ratio, Gokul et al. (1985), termed it as para-conglomerate, thus, not assigning any stratigraphic significance to it. The general stratigraphy of Goa Group is presented in Table 1. The Goa Group of rocks that rests on Anmod Ghat trondhjemitic gneiss of 3.3 Ga (Devaraju, et al., 2007), typically consists of a sequence of metasediments with metavolcanics at the base followed by a suite of clastic rocks that have suffered greenschist facies of metamorphism. These rocks are in-turn intruded by granitoids, layered complexes and mafic dykes. They are subdivided into two Groups, viz., the Barcem Group comprising the Barcem Formation and the Ponda Group consisting of the Sanvordem Formation, Bicholim Formation and the Vagheri Formation (Dessai, 2011).

The polymict para-conglomerate horizon under study is sheared and consists of stretched and flattened pebbles in a well foliated matrix (Rekha, et al., 2013a; Dessai, 2011). The clasts in the para-conglomerate vary from microscopic to boulder size (upto 80cm long). Their shape varies from being spherical to highly elliptical that are angular to well rounded. Their roundness increases with increase in size (Devaraju, et al., 2010). On an outcrop scale, many clasts display "mantled" morphologies with "beards" and "tails" of recrystallized matrix. Sigmoidal clasts are also very common with dextral sense of shear. Mylonitic foliation developed in this sheared horizon trends along NNW-SSE to N-S steeply dipping towards east with a stretched pebble lineation. The lineation defined by the pebbles has a plunge of 15° due SE (Gokul, et al., 1985). Th-U-Pb spot ages in monazites recovered from the matrix in the para-conglomerate indicates a date of 2458±34 - 2566±53 Ma while the monazites found within the tonalite clasts yield an age of 3128±60 Ma pointing towards Peninsular basement as the source of clasts to these para-conglomerates (Rekha, et al., 2013b). The para-conglomerate horizon in the study area is characterized by total obliteration of the primary bedding and is superimposed by a later pervasive mylonitic foliation that steeply dips towards east. The genesis of this mylonitic foliation and subsequently stretching of the pebbles corresponds to the 2^{nd} fold cycle that affected the Goa Group of rocks (Gokul, et al., 1985).

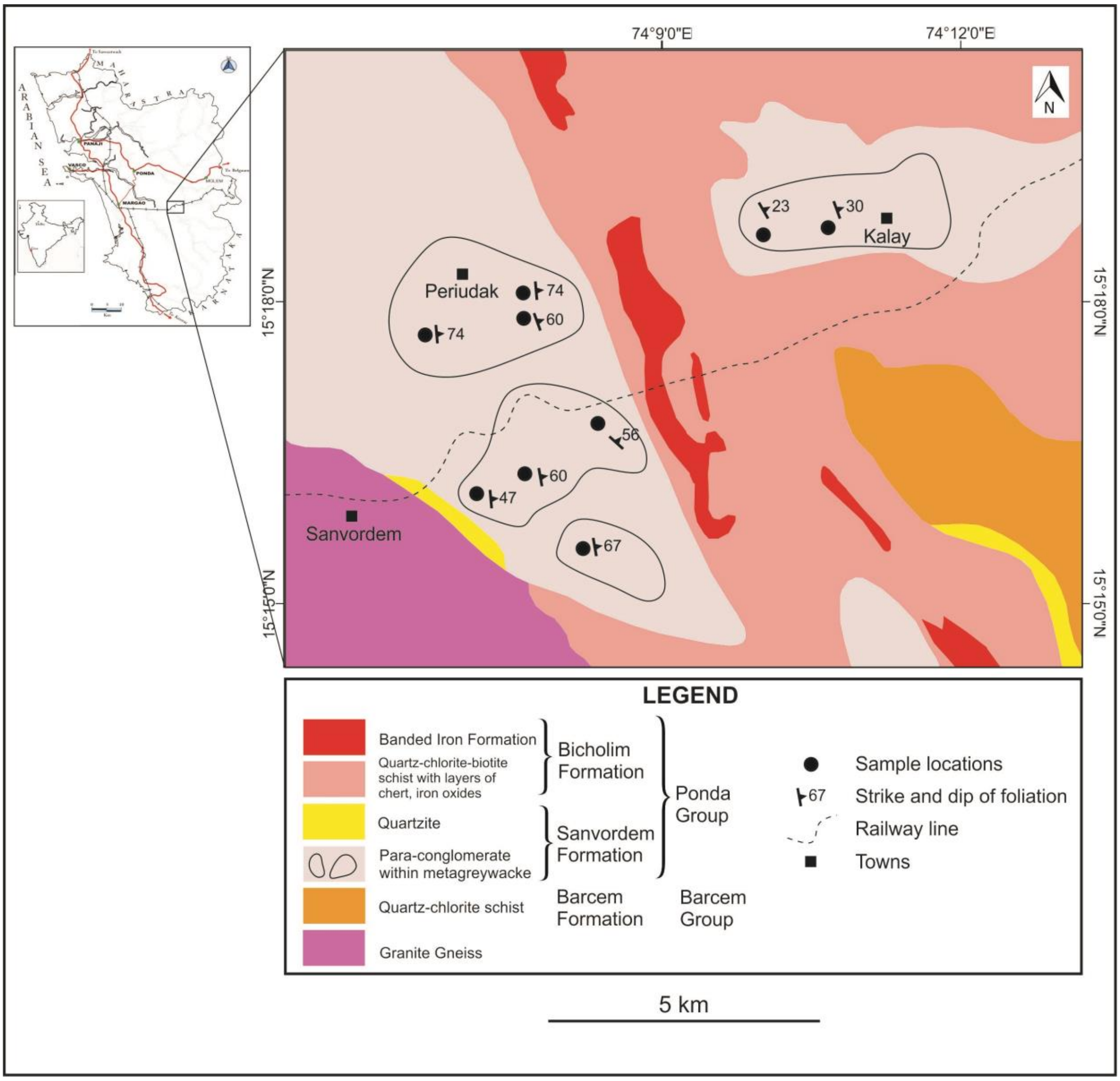

Figure 1: Simplified geological map of the study area. Modified after Sreeramachandra Rao, et al., (1996)

Table 1: Lithostratigraphic sequence of Goa Group (Modified after Dessai, 2011).

Rocks	Age/Formation	Lithology
Newer Intrusives	62.8±0.2 Ma[1]	Dolerite
Older Intrusives	Proterozoic	Metadolerite
Mafic-ultramafic layered complex	1644-1536[2]	Dunite-peridotite-gabbro complex and equivalents
Ponda group	Vagheri Formation	Metabasalt, argillite and metagreywacke
	Bicholim Formation	Banded ferrugenous quartzite, Manganeferous chert breccia, Limestone, Ferrugenous phyllite, Quartz-chlorite-amphibolite schist
	Sanvordem Formation (Para-conglomerate matrix 2458±34 to 2566±53 Ma[3])	Metagreywacke, Argillite, Quartzite, Para-conglomerate
~ ~ ~ ~ ~ ~ ~ ~ ~ ~ ~ ~ ~ ~ ~ ~ ~ ~ ~ ~	Unconformity	~ ~ ~ ~ ~ ~ ~ ~ ~ ~ ~ ~ ~ ~ ~ ~ ~ ~
Barcem Group	Barcem Formation	Metagabbro, Peridotite, talc-chlorite schist, Quartzite, Phyllite, Quartz Porphyry, Massive, schistose and vesicular metabasalt
~ ~ ~ ~ ~ ~ ~ ~ ~ ~ ~ ~ ~ ~ ~ ~ ~ ~ ~ ~	Unconformity	~ ~ ~ ~ ~ ~ ~ ~ ~ ~ ~ ~ ~ ~ ~ ~ ~ ~
Chandranath Granite Gneiss	2500±37 to 2619±37 Ma[3]	Granodiorite
Canacona Granite	2924±35 Ma[3]	Porphyritic potassic granite
Anmode Ghat trondhjemite gneiss	3138±35 Ma[3] 3300 Ma[4]	Basement: trondhjemite-tonalite-granodiorite

Adopted from [1]Widdowson, et al., 2000; [2]Ishwar-Kumar, et al., 2013; [3]Rekha et al., 2013b; [4]Devaraju et al., 2007

3. Petrography and Structures

The pebbles dominantly constitute of quartzite, tonalite, gneiss and occasional granite in biotite-chlorite matrix. The pebbles of quartzite consist entirely of interlocking medium to fine quartz grains. They show primary lamination and some of them exhibit micro scale graded bedding. Few mica grains are occasionally present. Pressure solution along quartz grain boundaries is abundantly seen.

Tonalite pebbles essentially consist of plagioclase, quartz, alkali feldspar with muscovite and biotite as accessory minerals. Plagioclase is often altered to a mixture of epidote and calcite and alkali feldspar is partly sericitized giving clouded appearance. Gneissic pebbles are dominated by a distinct gneissose banding and are in turn cut across by quartz veins. The Granite clasts are predominantly made up of alkali feldspar and quartz with biotite and plagioclase as accessory minerals. Myrmekitic intergrowth is often seen.

Microstructural observations are made from sections cut perpendicular to foliation and parallel to lineation, and presumably representing the XZ plane of finite strain. They are summarized as follows.

3.1 Quartz porphyroclasts

They are the most abundant, sometimes making up for most of the clasts in the rock. The constituent grains show large scale dynamic recrystallization, undulose extinction, subgrain formation, Grain Boundary Migration (GBM) and bulging recrystallization (BLG) (Figure 2a and 2b respectively). Quartz shares un-equilibrated phase boundaries with feldspars and other quartz grains. It also exhibits serrated to stylolitic grain boundaries that are a consequence of pressure solution. Occasionally quartz has recrystallized establishing planar grain contacts with other grains (Figure 2c). Quartz ribbons are formed closer to margins of the clast where the fragments are detached from the clast and dragged along foliation (Figure 2d). Recrystallized and remobilized veins of quartz with equilibrated grain contacts cut across the main mylonitic foliation and the tonalite clasts (Figure 2e-f) signifying their late stage formation.

3.2 Feldspar porphyroclasts

These comprise of both K-feldspar and plagioclase clasts that exhibit strong deformational evidence as most of the elongate or oval grains rotate in accordance to the shear direction to the east. Long plagioclase laths show clear evidence of brittle shattering as manifested in micro-faulted twin lamellae. They also show, though less frequently, as evidenced by bent lamellae (Figure 3a). K-feldspars forming myrmekites at their contact with plagioclase is a common phenomenon (Figure 3b). The grain boundaries are mostly smooth and rarely serrated.

3.3 Matrix

The matrix is mainly defined by crushed and partly recrystallized quartz, feldspar, biotite, chlorite and muscovite. Chlorite is found rimming biotite and is presumed to be a result of the breakdown of the latter. Sphene, epidote, zoisite/clinozoisite and tourmaline are common accessories. Larger lithoclasts show some degree of differentiation resulting in distinct domainal discontinuous to continuous cleavage with well-defined p- and q-domains (Figure 3c). In a few instances, the matrix is dominated by fine recrystallized calcite. Some biotite grains are preferentially oriented forming the fish structure.

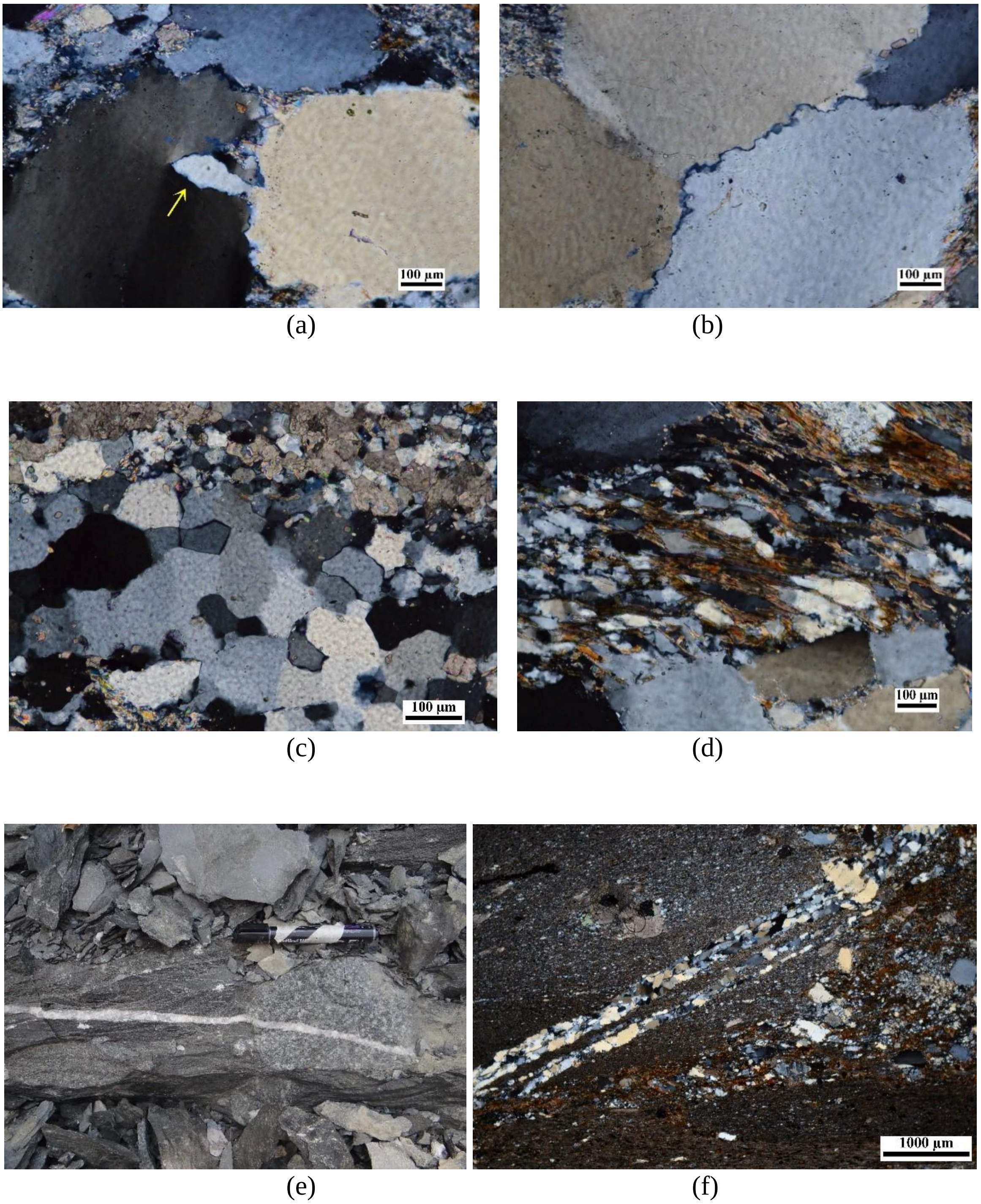

Figure 2: (a) Peninsula of quartz remain joined to the main body of grain by narrow isthmuses. The peninsulas are incipient new grains detaching from the parent grains by Grain Boundary Migration (GBM). (b) Serrated grain boundaries in quartz formed by grain boundary bulging (BLG) in a deformed quartzite clast. (c) Recrystallized grains of quartz with straight grain boundaries and the tendency of these contacts to make angles of 120o at triple junctions. (d) Monocrystalline quartz grains in a matrix of biotite detached from the clast (base of photo) are deformed by crystal-plastic deformation forming ribbons with sweeping undulose extinction. (e) and (f) Quartz remobilized as veins that cuts across the mylonitic foliation at a low angle. Note in (f) undulose extinction shown by subgrains with serrated contacts. Pen in (e) is 14.5cm across. Photographs a-d and e in cross-polarized light.

Where the matrix is dominantly biotite-chlorite, well defined crenulation cleavage has formed. The opaques also exhibit this feature (Figure 3d). Deformation of phyllosilicate dominated matrix foliation, particularly adjoining the clast, has produced kink bands (Figure 3e). In many cases micas anastomose around quartz and feldspar porphyroclasts (Figure 3f). Opaques,

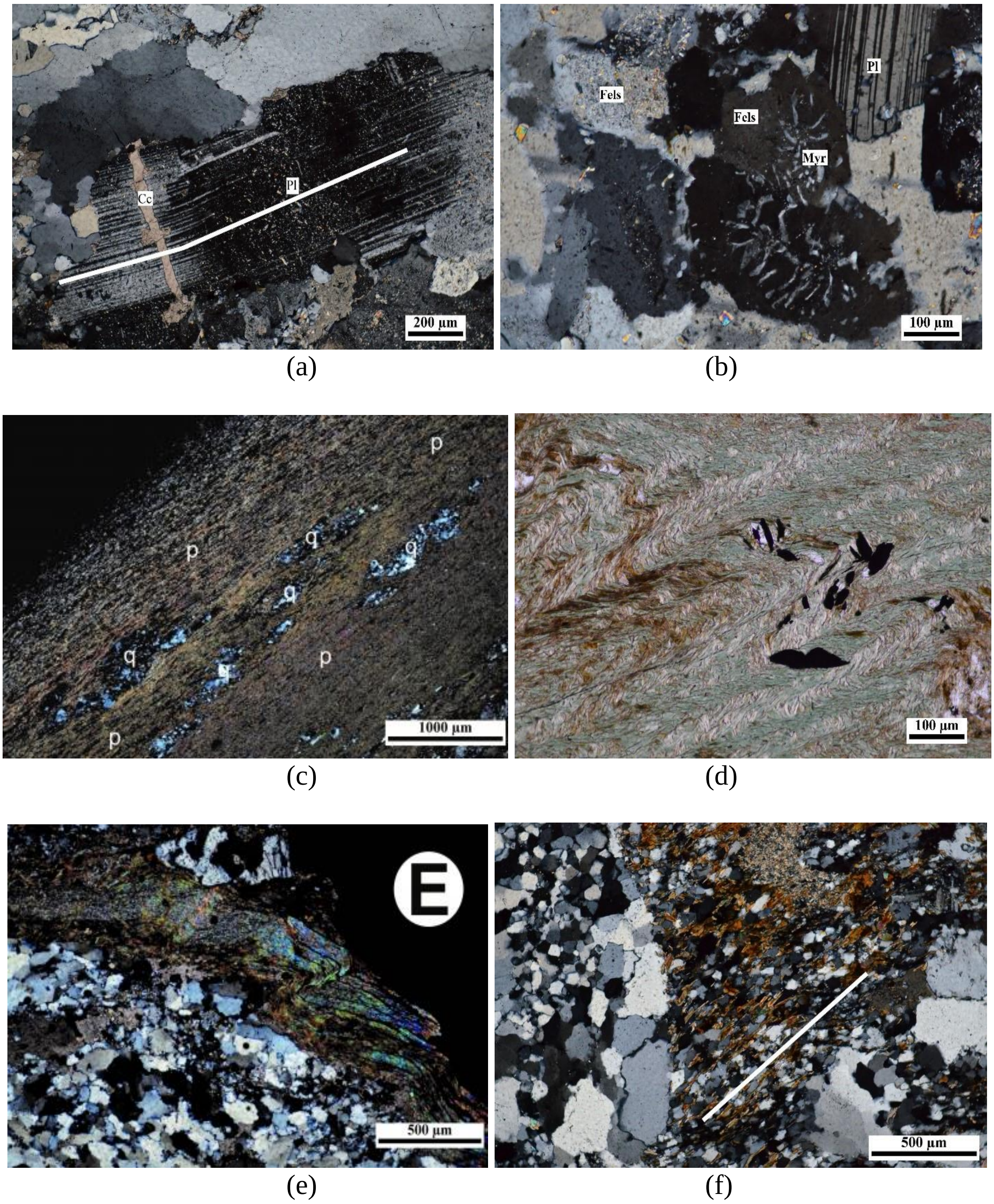

Figure 3: (a) Plagioclase (Pl) grain from a tonalite clast shows ductile bending of twin lamelle. Calcite (Cc) vein traverses the grain seen at bottom left. (b) Myrmekite forming replacing K-feldspar (Fels). (c) The quartzite lithoclasts have recrystallized into finer grained non-strained aggregates. (d) Crenulation cleavage defining S-C fabric in chlorite-

biotite matrix. C bands run diagonally from lower left to upper right and S bands are roughly orthogonal to the base of the photo. Note opaques too have been crenulated. (e) Biotite >> chlorite defined foliation adjacent to a quartzite clast (left part of the photo) has kinked. (f) Biotite defining foliation (white line) along with fine recrystallized quartz swerves around the quartzite clast (left of the photo). Photographs a-c and e-f in cross polarized light. Photograph d in plane-polarized light.

wherever present, are skeletal in outline and are intergrown with biotite, chlorite and quartz. Disoriented biotite and chlorite grains are also seen.

4. Shear Sense Indicators

Sections cut perpendicular to the foliation and parallel to lineation reveal asymmetric mantled porphyroclasts, mineral fish along with domainal cleavage, kink bands, micro-faults and pull-apart microstructures.

4.1 Mantled and sigmoidal porphyroclasts

Asymmetric mantled porphyroclasts (both litho- and mineral) are ubiquitously distributed (Figure 4a-d). They are mainly of σ-type with few being faulted along the midline (Figure 4e). Symmetric mantled clasts are also evenly distributed known as φ-type (Figure 4f). Mantles of these grains are formed by recrystallized quartz, feldspar and biotite flakes. The recrystallized tails exhibit stair stepping. Sigmoidal lithoclasts of quartzite are commonly seen in outcrops (Figure 5a). Recrystalllized tails in σ-type mantles exhibit stair stepping from which a dextral top-to-East (down) shear can be deciphered.

4.2 Micro-shears

These correspond to the brittle and observable displacements along the fracture planes affecting the quartz clasts (Figure 4d), calcite clasts and displacing the twin lamellae in plagioclase (Figure 5b-d). Microshears parallel to each other producing step like features are seen in plagioclase grains within the tonalite clasts (Figure 5c). Plagioclase commonly shows features indicative of brittle deformation.

4.3 Mineral fish

Mineral fish are lozenge shaped single crystal porphyroclasts in fine grained matrixes in mylonitised rocks (Ten Grotenhuis, et al., 2003). Mineral fish are the most common ductile micro-scale shear sense indicators. Ten Grotenhuis et al. (2003), classified mica or mineral fishes into 6 groups on the basis of their morphology and mechanism of formation. The observed mineral fishes can be conveniently divided into 2 broad morphologies (1) Parallelogram (2) Sigmoid (Figure 5e-f) which corroborate with the Top-to-East (Down) shear observed. The sigmoid fish are later sub classified as Steep sigmoid fish, Elongated sigmoid fish and Snake fish (Mukherjee, 2011) out of which Steep and elongated sigmoid fish are observed here (Figure 5f).

4.4 Other structures

The quartzite lithoclasts of abundantly show pinch and swell structure on the mega scale (Figure 6a). While a similar structure is seen in quartzite lithoclasts in micro scale where part of the lithoclast is stretched and dragged along foliation with dextral sense of shear (Figure 6b). Boudinage on micro- and megascopic scale is commonly seen in clasts of competent lithology and minerals. Pull-apart structures were first described in micro-scale by Hippertt, (1993), and Singh, (1999) and provides a comprehensive review on pull-aparts. Samanta, et al., (2002) describes type 1 pull aparts as having parallel displacements with maintenance of parallelism between the fractured walls of grains during movement. Here, type 1 pull apart structures are exhibited by plagioclase grains which are themselves a part of lithoclasts of tonalite (Figure 6c). Recrystallized flakes of biotite caught up in an inclined manner to the mylonitic foliation has been shredded along cleavage, folded across the cleavage as well as faulted along it (Figure 6d). A number of biotite grains within small lithoclasts of tonalites have behaved in a ductile manner commonly developing kinks (Figure 6e). It also shows effects of strain localization leading to tear apart along cleavage, both at tips as well as in the centre of the grain (Figure 7a-c). Remobilized calcitic solutions have formed anhedral grains throughout the rock. This calcite has been invariably deformed forming less common narrow to straight twins to wider twins that are very abundant where the width of twin lamellae is distinctly found to be >>1µm (Figure 7d).

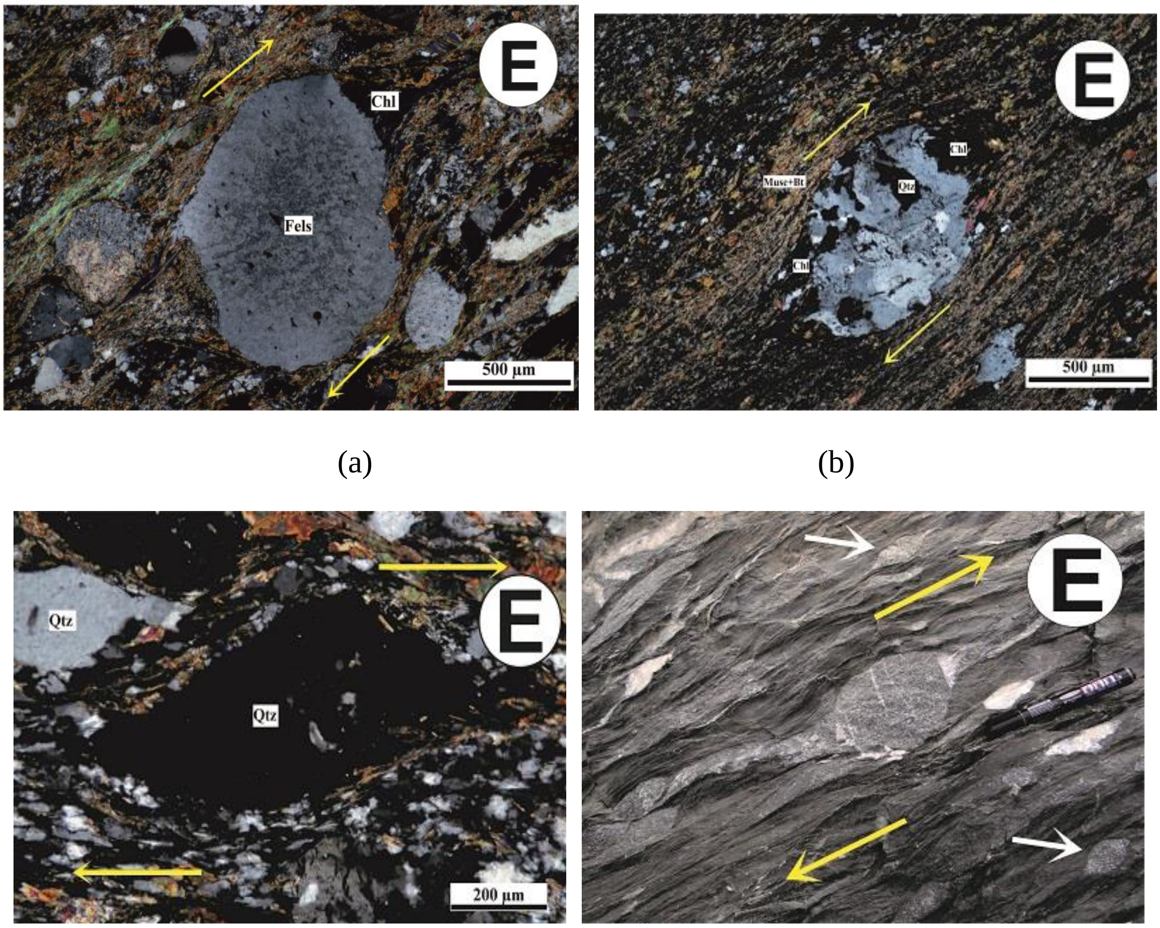

(a) (b)

(c) (d)

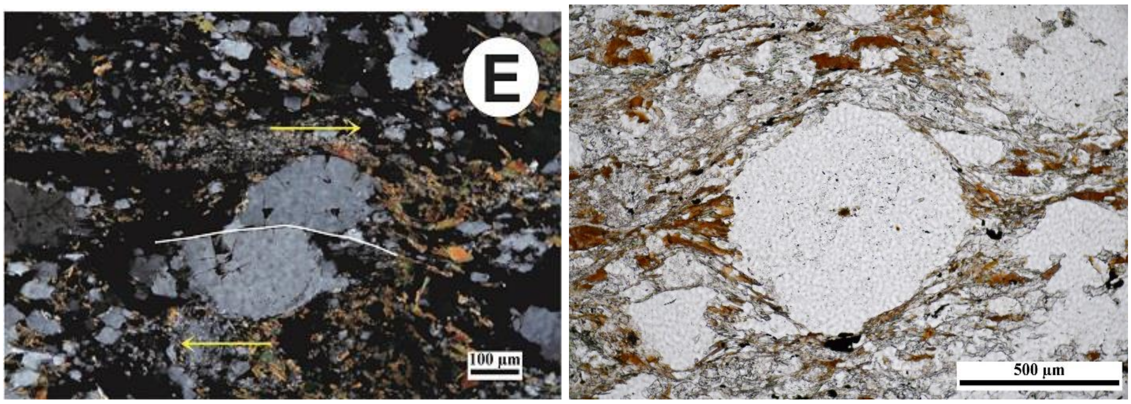

(e) (f)

Figure 4: (a) Porphyroclast of K-feldspar showing asymmetric strain shadow consisting of massive chlorite at its top end and mixture of biotite-muscovite at its bottom end. Dextral sense of shear. (b) Massive strain shadow made up of chlorite and less commonly biotite occurs on the sides of granite clast. Foliation is weakly developed in the strain shadow. Strain caps consisting of biotite have developed on the opposite sides of granitic clast, in the quarters oblique to the strain shadow. Dextral sense of shear. (c) Sigmoidal quartz clast that has a mantle of recrystallized quartz. It shows a dextral sense of shear. (d) Field photograph of a sigmoid granite clast with drawn out tails exhibiting pinch and swell. Dextral sense of shear. There are symmetrical φ-type clasts at the top center and bottom left of the photograph (white arrow). Pen is 14.5cm long (e) Faulted porphyroclast of quartz showing dextral shear sense. (f) Feldspar φ-type clast slightly rhomboidal in shape with symmetrical tails of biotite. Photographs a-c and e in cross polarized light. Photograph f in plane-polarized light.

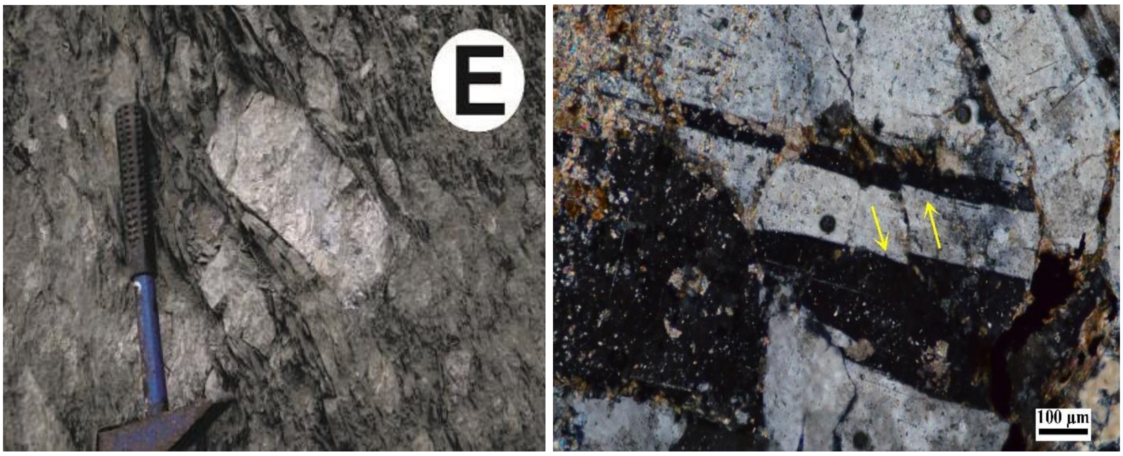

(a) (b)

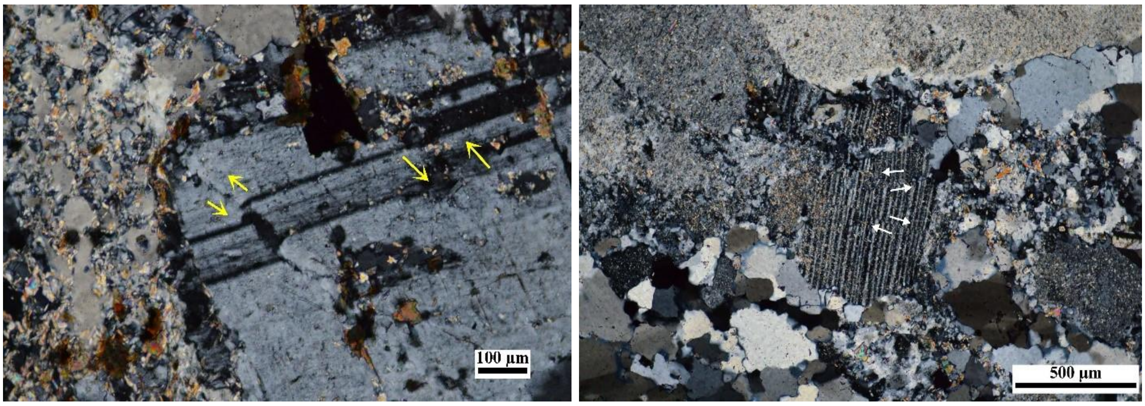

(c) (d)

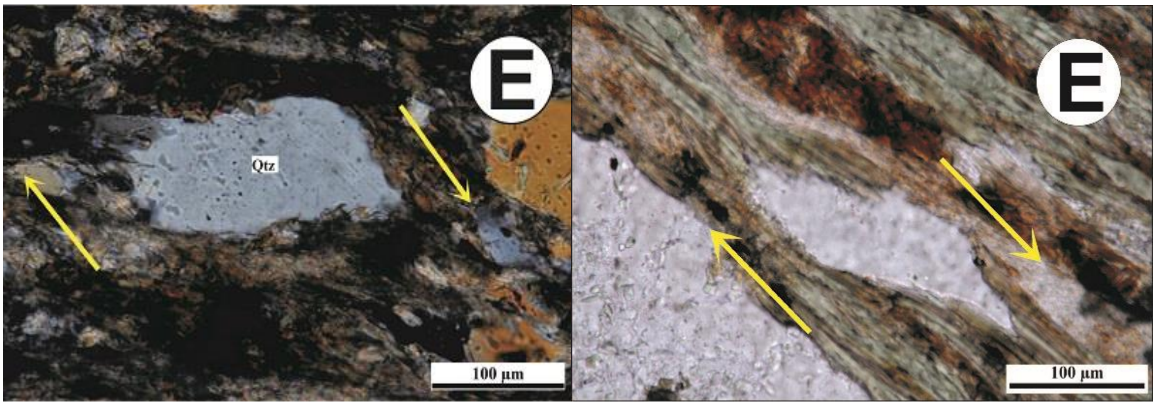

(e) (f)

Figure 5: (a) Sigmoidal quartzite clast. Hammer for scale. (b-c-d) Plagioclase grains within tonalite clasts shows effects of brittle deformation with the wrecking of twin lamelle in a series of faults. In (b), the plagioclase has altered to calcite within the fractures developed. In (c) Plagioclase within tonalite clast shows “step” faults in conjugate fractures with sinistral type of movement. (e) Parallelogram fish shown by quartz clast with its tips parallel to the mylonitic foliation. (f) Elongated sigmoid fish with sharp tips parallel to the mylonitic foliation. Both (e) and (f) display Top-to-East (Down) dextral sense of shear. Photographs b-e in cross-polarized light. Photograph f in plane-polarized light.

(a)

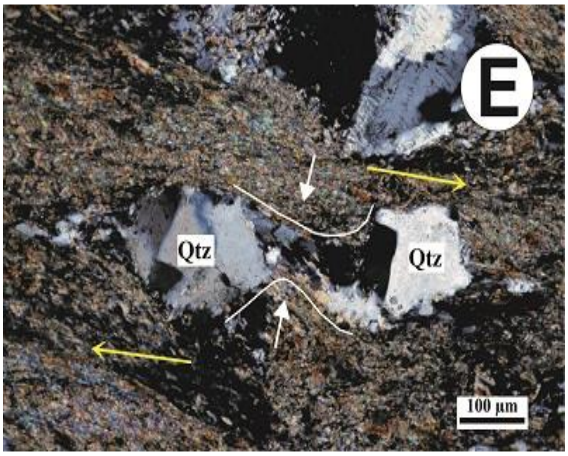

(b)

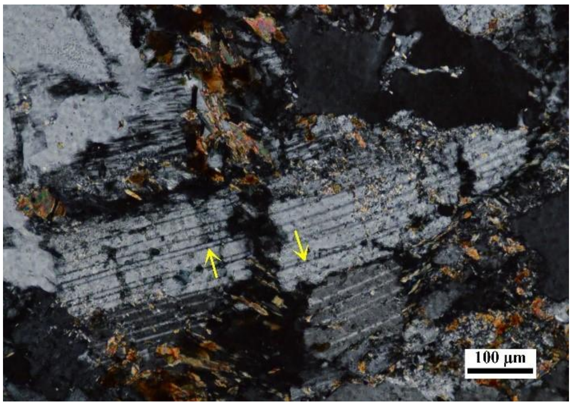

(c)

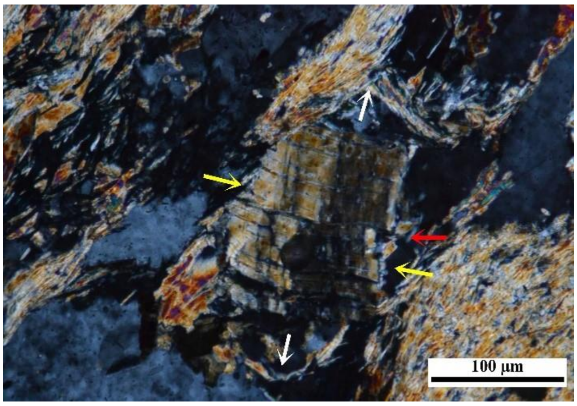

(d)

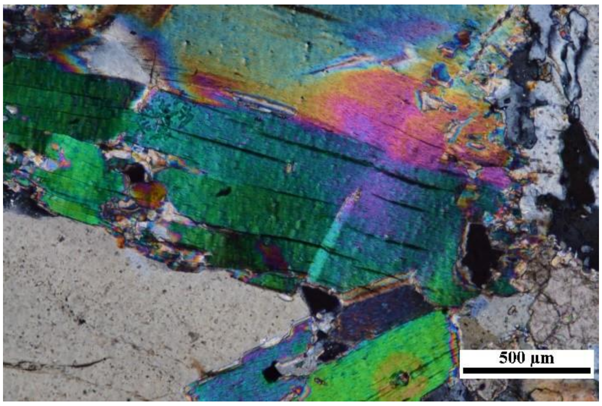

(e)

Figure 6: (a) Field photograph of quartzite lithoclast showing pinch and swell. Pen 14.5cm. (b) Part of quartzite lithoclast stretched along foliation exhibiting dextral Top-to-East (Down) sense of shear. (c) Plagioclase grain in tonalite lithoclast microfaulted and simultaneously pulled-apart (Type 1). (d) Complexly deformed biotite grain in the matrix. The grain has been faulted (yellow arrow), shredded and faulted along cleavages (white and red arrows). (e) Biotite grain within stressed tonalite clast shows an isolated kink band that tapers within the grain. Photographs b-e in cross polarized light.

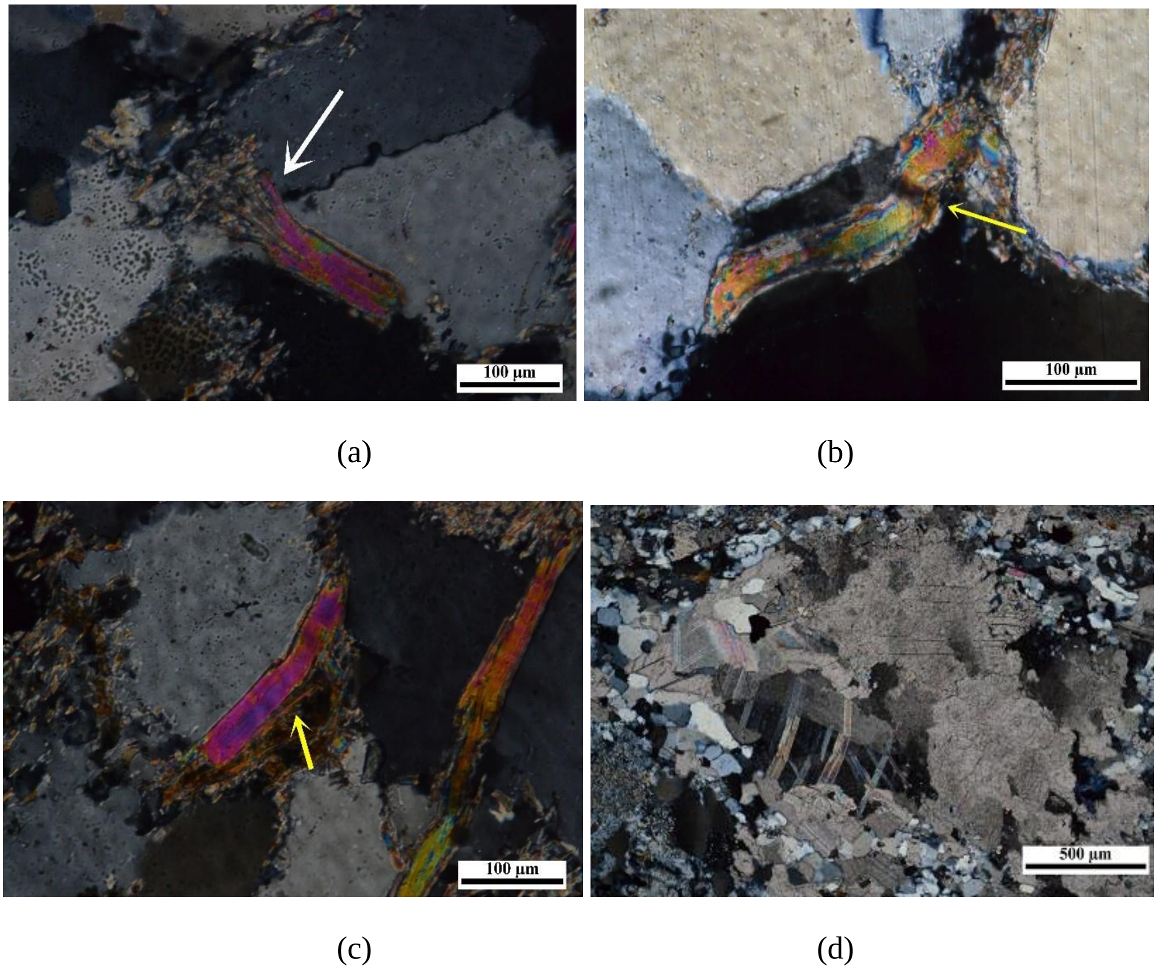

Figure 7: (a) Shredding of biotite (white arrow) along cleavage planes at tips. (b) Biotite kinked (yellow arrow) and bent for the entire length. (c) Biotite bent in the center and shredded along sides. (d) Deformation twins in calcite that are >1µm wide. All photomicrographs in cross polarized light.

5. Discussions and conclusion

The para-conglomerate of the Sanvordem Formation trending N-NNW to S-SSE has been sheared. The field as well as thin sections reveal variable intensity of ductile and brittle shearing, subsequent to mylonitization in the deformed rocks. Reported monazite spot dating from the matrix of para-conglomerate from elsewhere in the region denote an age of 2458±34 to 2566±56 Ma (Rekha, et al., 2013b). The foliation planes were formed during 2nd phase of folding of the Goa Group of rocks (Gokul, et al., 1985).

The deformation structures observed are summarized in Figure 8. Mylonitic structures and textures of mainly quartz, feldspar, plagioclase along with quartzite and tonalite lithoclasts within the para-conglomerates reveal an extensive deformation pattern. An array of deformation microstructures, all exhibiting dextral brittle-ductile shearing towards east characterize the mylonitic para-conglomerate. The σ-mantled porphyroclasts usually result from high differential stresses at the rim of isolated porphyroclast in the matrix. Type 1 parallel pull apart seen in long laths of plagioclase that are present in deformed tonalite lithoclast also conform to the same sense of shear. Quartz fish are relatively rare in mylonites, however, quartz porphyroclasts will only survive in a soft and usually fine-grained matrix (Ten Grotenhuis, et al., 2003). The parallelogram and sigmoidal types of quartz fish that are found in these para-conglomerates exhibit pronounced stair stepping dextrally towards east (Figure 8).

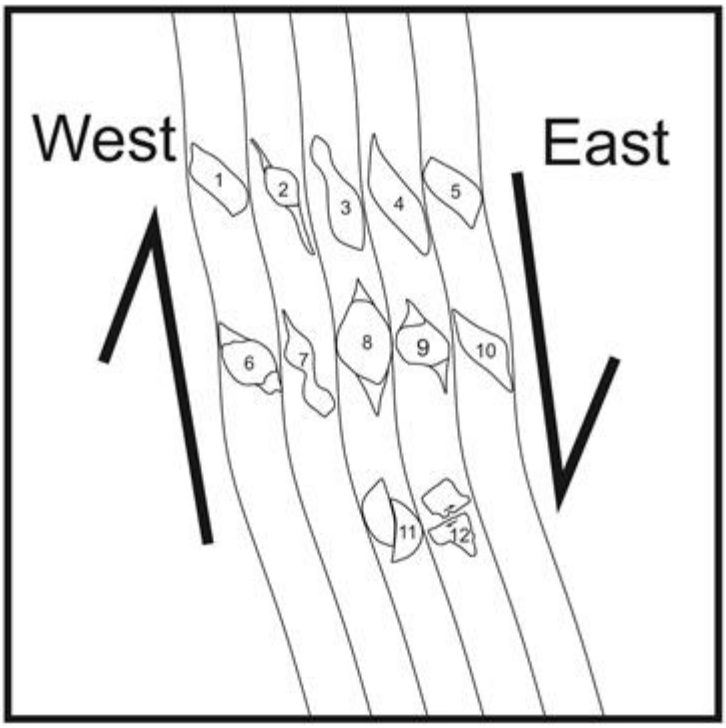

Figure 8: Schematic composite diagram of the microstructures in the para-conglomerate with numerous shear indicators showing dextral shear sense. (1) Figure 5a (2) Figure 4d (3) Figure 6a (4) Figure 5f (5) Figure 5e (6) Figure 4b (7) Figure 6b (8) Figure 4f (9) Figure 4a (10) Figure 4c (11) Figure 4e (12) Figure 6c

Temperature conditions can be estimated within the ductile shear zones from the presence of deformed minerals which are used as temperature gauges, whose behavior has been summarized in few studies e.g., Passchier & Trouw (2005), Simpson (1985) and Nyman, et al. (1992). The ductile deformation of the para-conglomerates is accompanied by recrystallization, grain boundary migration, grain size reduction and crystal-plastic deformation. Quartz, for most of the time, shows evidence of crystal-plastic deformation by the presence of undulose extinction, stylolitic grain boundaries, solution transfer of quartz and re-deposition as veins and formation of a variety of fish structures. Quartzite clasts occasionally show effects of brittle deformation in the form of microfaults. Among the feldspar clasts, the K-feldspars in the matrix form asymmetric mantled porphyroclasts with pressure shadows whereas undulose extinction, recrystallization and formation of myrmekites is restricted to the feldspars in contact with plagioclase or quartz. Plagioclase feldspars dominantly display brittle deformation. These include faulting of the twin lamelle along with rare pull apart structure. However, sometimes, ductile bending of plagioclase is also noticed within the lithoclasts of tonalite. Biotite displays effects of deformation in the form of kinks, bending of grains, undulose extinction, splaying of tips along cleavage and faulting accompanied with folding of the grain; all these evidences indicate the temperature of deformation over 300° C. However, dynamic recrystallization of quartz as bulging and grain boundary migration, formation of prismatic subgrains, and formation of ribbons indicate the temperature of deformation to be as high as 450° C (Passchier & Trouw, 2005).

The twin lamelle in calcite have been suggested as a temperature gauge (Passchier & Trouw, 2005 and references therein). Calcite forms narrow straight twins to wider twins in the matrix of para-conglomerate where it is ubiquitously found as recrystallized aggregates. These are ascribed to Type I and Type II twins respectively. Recrystallized calcite having narrow straight twins (less than 1 µm wide – Type I of Burkhard (1993) indicate temperatures below 200° C. However, wider twins (Type II > 1 µm) dominate above 200° C up to 300° C (Groshong, et al. (1984); Rowe & Rutter (1990); Evans & Dunne (1991); Ferill (1991); Ferill et al. (2004) are abundantly seen.

Hence the microstructural features constrain the temperature of mylonitization of para-conglomerates from as low as 200° C to up high as 450° C. This temperature estimate is bolstered by the characteristic mineralogy present in the matrix to the greenschist facies metamorphic conditions.

6. Acknowledgements

The authors are grateful to Prof. K. Mahender, Head, Department of Earth Science, Goa University for his encouragement and support to publish this work. The authors also acknowledge Prof. A. G. Chachadi (Retd) for his support. The departmental facilities used during this work are duly acknowledged. We thank Dr. Mriganka Ghatak, Superintending Geologist, LHIM Division, Geological Survey of India for his thoughtful review on the earlier version of the manuscript. The authors also thank Dr. A. Viegas and Dr. S. Ganguly, Department of Earth Science, Goa University and Dr Sayandeep Banerjee, Department of Geology, Banaras Hindu University for their valuable suggestions during preparation of the manuscript.

7. References

1. Bak, J., Korstgard, J. & Sorensen, K., (1975), A major shear zone within the Nagssugtoquidian of west Greenland. Tectonophysics, 27, pp 191-209.

2. Burkhard, M., (1993), Calcite twins, their geometry, appearance and significance as stress-strain markers and indicators of tectonic regime: a review. Journal of Structural Geology, 15(3-5), pp 351-368.

3. Dessai, A. G., (2011), The geology of Goa Group: revisited. Journal Geological Society of India, 78, pp 233-242.

4. Devaraju, T. C., Huhma, H. C., Kaukonen, R. J. & Alapeiti, T. T., (2007), Petrology, geochemistry, model Sm-Nd ages and petrogenesis of the granitoids of the northern block of western Dharwar craton. Journal geological society of India, 70, pp 889-911.

5. Devaraju, T. C. et al., (2010), Petrology and geochemistry of greywackes from Goa-Dharwar sector, western Dharwar craton: implications for volcanoclastic origin. Journal geological society of India, 75(3), pp 465-487.

6. Evans, M. A. & Dunne, W. M., (1991), Strain factorization and partitioning in the North Mountain thrust sheet, central Appalachians, USA. Journal of structural geology, 13(1), pp 21-35.

7. Ferill, D. A., (1991), Calcite twin widths and intensities as metamorphic indicators in natural low-temperature deformation of limestone. Journal of Structural geology, 13(6), pp 667-676.

8. Ferill, D., Morris A. P., Evans M. A., Burkhard M., Groshong Jr. R. H., Onasch C. M., (2004), Calcite twin morphology: a low-temperature deformation geothermometer. Journal of structural geology, 26(8), pp. 1521-1529.

9. Gadgil, R., Miranda, M. A., Sawant-Dessai, K. K. & Viswanath, T. A., (2015), Petrography, meso- and microstructures of deformed paraconglomerate, Sanvordem Formation, Goa Group. In: National seminar on recent advances in research on Precambrian Terrains of India Abstracts. University of Mysore.

10. Gokul, A. R., Srinivasan, M. D., Gopalkrishnan, K. & Vishwanathan, L. S., (1985), Stratigraphy and structure of Goa. Geological survey of India, pp. 1-13.

11. Groshong, Jr. R. H., Teufel, L. W. & Gasteiger, C., (1984), Precision and accuracy of the calcite strain-gauge technique. Geological society of america bulletin, 95(3), pp 357-363.

12. Hanmer, S., (1988), Great Slave Lake Shear Zone, Canadian Shield: reconstructed vertical profile of a crustal-scale fault zone. Tectonophysics, 149(3-4), pp. 245-264.

13. Hippertt, J. f. M., (1993), ‘V’ pull-apart microstructures: a new shear sense indicator. Journal of Structural Geology, 15(12), pp 1393-1403.

14. Ishwar-Kumar, Windley B. F., Horie K., Kato T, Hokada T., Itaya T., Yagi K., Gouzu C. & Sajeev K., (2013), A Rodinian suture in western India: new insights on India-Madagascar correlations. Precambrian Research, 236, pp 227-251.

15. Mukherjee, S., (2011), Mineral fish: their morphological classification, usefulness as shear sense indicators and genesis. International journal of earth science (Geol. Rundsch), 100(6), pp. 1303-1314.

16. Nyman, M. W., Law, R. D. & Smelik, E. A., (1992), Cataclastic deformation for the development of core mantle structures in amphibole. Geology, 20(5), pp 455-458.

17. Ojakangas, R. W., Srinivasan R., Hegde V. S., Chandrakant S. M., and Srikantia S. V., (2014), The Talya conglomerate: an Archean (~2.7 Ga) glaciomarine formation, western Dharwar Craton, southern India. Current science, 106(3), pp 387-396.

18. Passchier, C. W. & Trouw, R. A. J., (2005), Microtectonics. 2nd Edition ed. :Springer.

19. Ramsay, J. G., (1967), Folding and fracturing of rocks. New York: McGraw Hill.

20. Ramsay, J. G., 1980. Shear zone geometry: a review. Journal of structural geology, 2(1-2), pp 83-99.

21. Ramsay, J. G. & Graham, R. H., (1970), Strain variations in shear belts. Canadian Journal of earth sciences, 7(3), pp 786-813.

22. Rekha, S., Bhattacharya A. & Viswanath, T. A., (2013a), Microporosity linked fluid focussing and monazite instability in greenschist facies para-conglomerates, western India. Geochimica et Cosmochimica Acta, 105, pp 187-205.

23. Rekha, S., Viswanath, T. A., Bhattacharya, A. & Prabhakar, N., (2013b), Meso/Neoarchean crustal domains along the north Konkan coast, western India: The Western Dharwar Craton and the Antongil-Masora Block (NE Madagascar) connection. Precambrian research, 233, pp 316-336.

24. Rowe, K. J. & Rutter, E. H., (1990), Paleostress estimation using calcite twinning: experimental calibration and application to nature. Journal of structural geology, 12(1), pp 1-18.

25. Samanta, S. K., Mandal, N. & Chakraborty, C., (2002), Development of different types of pull-apart microstructures in mylonites: an experimental investigation. Journal of structural geology, 24(8), pp 1345-1355.

26. Simpson, C., (1985), Deformation of granitic rocks across the brittle ductile transition. Journal of Structural Geology, 7(5), pp 503-511.

27. Singh, K., (1999), Pull apart microstructures in feldspar from Chail Thrust Zone, Dhauladhar Range, Western Himachal Pradesh. In: A. K. Jain & R. M. Manickavasagam, eds. Geodynamics of the NW Himalaya. Gondwana research group memoir. Osaka, pp 117-123.

28. Sreeramachandra Rao, K.; Murthy, T. S. S.; Ramakrishna, T. L.; Janardhan, K.; Sundaram, V., (1996), Geological and mineral map of Goa (1:1,25,000). Geological Survey of India Publication.

29. Ten Grotenhuis, S. M., Trouw, R. A. J. & Passchier, C. W., (2003), Evolution of mica fish in mylonitic rocks. Tectonophysics, 372(1-2), pp 1-21.

30. Widdowson, M., Pringle, M. S. & Fernandez, O. A., (2000), A post K-T boundary (early Palaeocene) age for Deccan type feeder dykes, Goa, India. Journal of petrology, 41(7), pp 1177-1194.